Centrosome amplification increases single-cell branching in post-mitotic cells

Delia Ricolo[1,2], Myrto Deligiannaki[1,3], Jordi Casanova[1,2] and Sofia J. Araújo[1,2*]

[1]Institut de Biologia Molecular de Barcelona (IBMB-CSIC), Parc Cientific de Barcelona, C. Baldiri Reixac 10, 08028 Barcelona, Spain

[2]Institute for Research in Biomedicine (IRB Barcelona), The Barcelona Institute of Science and Technology, C. Baldiri Reixac 10, 08028 Barcelona, Spain

[3]Current address: Gene Center, Department of Biochemistry, Center of Protein Science CIPSM, Ludwig-Maximilians University, Feodor-Lynen-Str. 25, Munich 81377, Germany

[*]Corresponding author. EMAIL: sarbmc@ibmb.csic.es FAX: +34934034979

Keywords: centrosome; centriole; Rca1; Emi1; sas-4; lumen; subcellular; branching; Drosophila

Running title: centrosomes in branching

Summary

Centrosome amplification is a hallmark of cancer although we are still far from understanding how this process affects tumourigenesis [1, 2]. Besides the contribution of supernumerary centrosomes to mitotic defects, their biological effects in the post-mitotic cell are not well-known. Here we exploit the effects of centrosome amplification in post-mitotic cells during single cell branching. We show that *Drosophila* tracheal cells with extra centrosomes branch more than wild-type cells. We found that mutations in *Rca1* and *CycA* affect subcellular branching, causing tracheal tip cells to form more than one subcellular lumen. We show that *Rca1* and *CycA* post-mitotic cells have supernumerary centrosomes and that other mutant conditions that increase centrosome number also show excess of subcellular lumen branching. Furthermore, we show that *de novo* lumen formation is impaired in mutant embryos with less centrioles. The data presented here define a requirement for the centrosome as a microtubule-organizing center (MTOC) for the initiation of subcellular lumen formation. We propose that centrosomes are necessary to drive subcellular lumen formation. In addition, centrosome amplification increases single-cell branching, a process parallel to capillary sprouting in blood vessels [3]. These results shed new light on how centrosomes can contribute to pathology independently of mitotic defects.

Results

Regulator of cyclin A1 (*Rca1*) is required for the modulation of subcellular branching

In *Drosophila*, tracheal terminal cells (TCs) are formed during embryogenesis and they branch extensively during larval stages. During embryonic development, they form unicellular branches by generating a cytoplasmic extension and a concurrent lumen in the cytoplasm (Figure 1A, B). This so-called intracellular or subcellular lumen [3, 4] arises by *de novo* growth of an apical membrane toward the inside of the cell, a process which depends on cytoplasmic extension, asymmetric actin accumulation, microtubule (MT) network organization, and vesicle trafficking guided by the cytoskeleton [5-7]. However, the detailed molecular mechanisms by which a seamless lumen forms and multiple subcellular branches are generated inside a single cell are still not well understood. With this purpose, we started by searching for TC lumen bifurcations within a collection of tracheal developmental mutants generated in an EMS screen. While many of the mutants displayed luminal bifurcations as a result of extra TCs [8], we identified one complementation group (alleles G012 and GA134) where bifurcations arose inside the TCs (Figure 1C, D). Mutants belonging to this group failed to complement previously reported *Regulator of cyclin A1* (*Rca1*^{IX} and *Rca1*^{2}) alleles [9, 10]. These mutant alleles and all transheterozygous combinations also showed the same subcellular branching phenotype (Figure 1E, F and Figure S1C, F, L). *Rca1* is the *Drosophila* homolog of vertebrate Emi1 and a regulator of APC/C activity at various stages of the cell cycle [9, 11]. It shows high and ubiquitous expression

during early embryonic development, this high expression becoming restricted to proliferating cells after stage 13 [12]. Rca1 is required for both mitotic and meiotic cell cycle progression, and *Rca1* mutants arrest in G2 of embryonic cell cycle 16 with lower numbers of cells than the wt ([12] and modENCODE) [13]). However, this arrest is not the cause of *Rca1* mutant subcellular branching phenotypes, since other mutant conditions that induce the same cell-cycle arrest, such as *fzy* mutants [14], do not show TC bifurcations (Figure S1H). *Rca1* expression in tracheal cells was sufficient to restore the normal branching pattern autonomously (81%, n=32, Figure S1J, M). Furthermore, *Rca1* knockdown in tracheal cells was enough to generate TC bifurcations (in 47% of embryos, n=17, Figure 1E,F and S1K, L). These results indicate that Rca1 in differentiated tracheal TCs serves to regulate subcellular branching events.

Rca1 mutations expand the subcellular branching machinery

From early developmental stages, *Rca1* subcellular TC lumen formation followed the reported normal progression (Figure 1G,H) [5]. However, it was also apparent early on that these events were duplicated within the cytoplasm (Figure 1H and Movie S1) an observation corroborated by further characterization, using various cell markers. *Rca1* mutant TCs that showed excess subcellular branching extended cytoplasmic protrusions and grew a new apical membrane and subcellular chitin lumen accordingly (Figure 1H and I, J, N, O).

To visualize the dynamics of subcellular apical membrane formation in living embryos, we used a Baz/Par3-YFP construct driven by a trachea-specific line. As previously reported for dorsal branch (DB) TCs [5], subcellular lumen

formation in the wt ganglionic branch (GB) TCs appeared as a continuous process of sprouting from the apical side of the TC (Figure 1 G and Movies S1 and S2). In these wt TCs, new membrane was added to the lumen of the principal network at the junction and continued in the direction of cell elongation (Figure 1G and Movie S1). In *Rca1* mutant TCs, this membrane addition started as a double lumen from the apical junction and continued to extend as two lumina as the TC extended (Figure 1H and Movie S1). Each of the extending cytoplasmatic protrusions accumulated actin asymetrically at the tip, as detected by moesin, an F-actin binding protein (Figure 1 K, P). Interestingly, detailed analysis of *Rca1* mutant TCs for constituents of the aPKC/Par6/Baz at early seamless lumen growth stages indicated that these components accumulate apically at higher levels than in wt TCs (Figure 1L, M, Q, R).

CycA mutations induce similar subcellular branching phenotypes to _Rca1_

Rca1 positively regulates Cyclin A (CycA) levels by inhibiting APC/C activity [9, 12]. In *Rca1* mutants, CycA is degraded through APC/C-dependent proteolysis. We therefore addressed whether the *CycA* null mutant phenotype showed the same subcellular branching phenotypes as *Rca1*. Like *Rca1*, *CycA* mutant TCs displayed luminal bifurcations (Figure 1T, U, V). However, they also have cell-cycle phenotypes, lower numbers of tracheal cells [15, 16] and morphogenetic defects [17]. CycB was also found to be degraded prematurely in *Rca1* mutants [9]; however, whilst *CycB* mutants have cell-cycle defects they did not show subcellular branching phenotypes (Figure S1N-P). As previously concluded from the analysis of *fzy* mutants, the CycB results are consistent with the

subcellular branching phenotypes present in *Rca1* and *CycA* mutants not being directly attributable to the mitotic arrest in embryonic cell cycles.

Rca1 and *CycA* mutant cells have supernumerary centrosomes

What could the function of two so-called mitotic proteins in differentiation be? It is worth mentioning that in the developing tracheal system, once placodes start invagination no further cell division occurs. Therefore, the effect of Rca1 and CycA in the regulation of subcellular branching is most likely a post-mitotic function/effect of these mitotic proteins.

Subcellular lumen formation depends on a mechanism based on MT network organization [3, 5]. Therefore we wondered whether: (i) *Rca1* and *CycA* mutations affect the MT network and (ii) if changes in the MT network might be responsible for the extra subcellular lumen phenotypes.

Both Rca1 and CycA modulate the activity of APC/C [9, 11, 18-20]. Moreover, oscillation of APC/C activity provides an additional mechanism for coupling the centrosome duplication cycle with replication [18]. The centrosome is the major MT organizing center (MTOC) of cells, and centrosomes play a crucial role in the maintenance of cell polarity and cytoplasmic architecture [21]. Therefore, we asked whether *Rca1* and *CycA* mutants showed aberrant centrosome numbers.

We first quantified centrosome numbers in wt and *Rca1* mutant TCs. We detected an average of 2.3 ± 0.5 centrosomes per TC in the wt (n=33) and 3.8 ± 0.6 centrosomes per TC in *Rca1* mutants (n=42) (Figure 2A, B). In wt and *Rca1* TCs, centrosomes localized at the apical side of the TC at embryonic stage 14 (72% in wt, n=33 and 69% in *Rca1*, n=42) (Figure 4A,B). Centrosome number was variable between cells in the same mutant embryo.

Due to the technical difficulties of quantifying centrosome numbers in multicellular tissues and to confirm the results above, we quantified the numbers of centrosomes in *Rca1* and *CycA* mutant cells in culture. To do so, we performed RNAi of both *Rca1* and *CycA* in S2 cells. An increment in centrosome number was detected after either *Rca1* or *CycA* downregulation (Figure 2C, D). As controls we used *slmb* and *SAK/PLK4* that have been reported to increase and decrease centrosome number, respectively [22-24]. RNAi of *slimb* in the same conditions resulted in a similar increase in the proportion of cells with more than two centrioles, and RNAi of SAK/PLK4 led to a reduction in the number of cells with more than two centrioles (Figure 2C, D).

Centrosome amplification leads to extra subcellular branching

To examine whether the supernumerary centrosomes in *Rca1* and *CycA* mutants might be the cause leading to extra subcellular branching, we asked if we could get a similar phenotype by changing centrosome numbers by a different mechanism.

We first examined subcellular branching in *slimb* (*slmb*) embryos. Slmb is directly involved in centrosome amplification through the degradation of SAK/Plk4 [23, 25]. In *slmb* loss-of-function conditions, there is a high proportion of cells with more than two centrosomes [23]. The same effect is achieved when a non-degradable form of SAK, SAK-ND, is expressed in *Drosophila* cells [23]. We detected extra subcellular branching in *slmb* tracheal TCs (Figure 3B, G and S2B, F), thereby corroborating our hypothesis that higher numbers of centrosomes lead to extra subcellular branching events. In addition, we observed extra subcellular branching in TCs expressing SAK-ND (Figure 3C, G

and S2C, F). Of note, although SAK-ND was overexpressed in all tracheal cells by means of a *btl* driver, we detected luminal bifurcations only in the TCs. This result is similar to that obtained by overexpressing SAK-ND only in tracheal TCs (Figure S2D, E).

Since branching is physiologically induced upon overactivation of the FGF pathway, we also addressed whether centrosome amplification was required in these conditions. However, under conditions of FGFR overactivation, we mainly found GB branching as a result of higher numbers of TCs and not as a result of more subcellular lumina generation (Figure S3 A). In addition, in all TCs analysed under conditions of FGFR overactivation (n=16) we could not detect any supernumerary centrosomes (Figure S3 D,E). This suggests that subcellular lumen branching upon overactivation of FGFR does not seem to be dependent on centrosome amplification, at least during embryonic stages.

If extra centrosomes lead to luminal bifurcations in tracheal TCs, then a reduction in centrosome number might impair TC subcellular lumen formation. Sas-4 protein is essential for centriole replication in *Drosophila* [26]. *Sas-4* mutants gradually lose centrioles during embryonic development, such that by stage 15-16 centrioles are no longer detected in 50-80% of cells [26]. According to our hypothesis that centrosomes play a role in subcellular lumen formation, we detected that 88% of *sas*-4 mutants analysed had defects in TC subcellular lumen generation, quantified as at least one TC without subcellular lumen, despite high variability in the penetrance of the phenotypes (n=17 embryos, Figure 3E and S2G, I-L). Indeed, in *sas-4* mutant embryos we could detect TCs with 0, 1 and 2 centrosomes (Figure S2 J-L and P) and we could correlate the formation of a subcellular TC lumen only with the presence of 2 centrosomes

(n=29, Figure S2 L, Q). Furthermore, *sas-4* mutations rescued the *Rca1* bifurcation phenotype (Figure 3F, G and S2F, H, M-O), despite the same variability in centrosome number (Figure S2 P), suggesting that *sas-4* mutations prevent the generation of supernumerary centrosomes in *Rca1* mutant TCs. Taken together these data support a direct role for centrosomes in subcellular lumen formation.

Centrosomes are MTOCs during TC lumen initiation

We detected that centrosomes localize apically, near the cell-cell junction, in both wt and *Rca1* mutant TC (Figure 4A-F and S4C,D and Movie S3). In addition, there is a close relationship between localization of the centrosome pair in the wild-type and the site of initiation of luminal extension (Figure 4 E and Movie S3). In *Rca1* mutant TC the supernumerary centrosomes also localize apically in close contact with the extending bifurcated lumina (Figure 4 F inset and Movie S3).

The centrosome is the major MTOC in dividing and many postmitotic differentiated cells. However, in other cell types, MTOC function is reassigned from the centrosome to non-centrosomal sites [27]. In particular, in tracheal multicellular tubes, MT reorganization is coupled to relocalization of the MTOC components from the centrosome to the apical luminal cell domain [28]. We therefore questioned whether TC centrosomes were active as MTOCs. We observed stable acetylated MTs extending from these centrosomes (Figure 4G). In the wt, MT bundles emanate from near the cell-cell apical junction to the periphery of the TC [5]. We detected that these microtubules emanate from the centrosomal site (Figure 4G). In *Rca1* TCs, the supranumerary centrosomes

were also observed in apical positions, where they associated with MTs (Figure 4H). MTs are nucleated and anchored by the microtubule nucleator γ-tubulin (γ-tub), which is embedded within the pericentriolar material (PCM) of the centrosome [29]. We found that the apically localized centrosomes of wt and *Rca1* TCs accumulated γ-tub, thereby confirming their role as active MTOCs during subcellular lumen initiation (Figure 4I, J). We complemented these results with time-lapse imaging of EB1 and Asl in wt TCs (Movie S4 and Figure S4 E). In a second approach, we used a cold treatment assay, which is reversible and allows the evaluation of both MT disassembly and reassembly [28]. After 6 h at 4°C, MT fibers are depolymerized in TCs of wt and *Rca1* mutants (Fig. 4L, P). Upon recovery for 2 min at room temperature (RT), MTs can be detected at the centrosomal sites (Fig. 4M, Q). Together, these results suggest that TC centrosomes are active MTOCs during subcellular lumen initiation.

Discussion

Here we report a new role for the centrosome in cytoskeletal remodeling during subcellular lumen formation. Our findings demonstrate that centrosomes are essential for the formation of tracheal TC subcellular lumina and that centrosome number is a key determinant of the number of subcellular lumina.

The graphical representation of our findings on the involvement of centrosomes in subcellular lumen formation in tracheal TCs is shown in Figure 4S, T. In wt TCs, two centrosomes localize apically to the junction of the TC with the stalk cell. There, they become MTOCs and provide the cytoskeletal structure necessary to start forming the ingrowing subcellular lumen (Figure 4S). The

MTs that emanate from this centrosome-pair grow towards the basolateral membrane (tip) of the TC, forming two tracks through which membrane can be delivered and the new lumen built (Figure 4S and S4A,B). In TCs with supernumerary centrosomes, extra apically localized MTOCs are active, leading to extra growing MT-tracks and the consequent formation of luminal bifurcations (Figure 4T).

We observed higher levels of apical complex proteins such as Baz and aPKC in *Rca1* mutant TCs (Figure 1Q,R), and these TCs had supernumerary centrosomes that localized apically (Figure 4D,F). Therefore, our data suggest that a higher-order complex formed by centrosomes and apical complex proteins is required to achieve the polarization event that triggers subcellular lumen initiation. Accordingly, previous studies have shown a close association between Baz, aPKC and centrosomal proteins during cytoplasmic polarization events [30-33]. We propose that the structure formed by the centrosome pair, which localizes apically in wt TCs, is necessary for the organized expansion of the apical plasma membrane towards the tip of the cell. This notion is in agreement with our observations that subcellular lumina in cells lacking this centrosome pair do not extend within the TC (Figure 3E and S2J). On the basis of our results and observations reported in cells with similar subcellular lumina, we propose that this model can be generalized to other species such as *C. elegans* [34] and mouse [35].

We show that centrosome amplification in all tracheal cells increases branching of only the TCs. This suggests that centrosomes are particularly important as MTOCs in single-cell *de novo* lumen formation. The main difference between these and non-centrosomal complex arrangements of MTs, such as those

present in *Drosophila* embryonic tracheal cells with non-subcellular lumina [28] or *C. elegans* embryonic intestinal cells [36], is the necessity for symmetry breaking within the cytoplasm, the need for rapid and radical cytoskeletal remodeling and the generation of new intracellular structures. This is particularly important during periods in which rapid subcellular lumen formation is required, such as rapid organ growth or angiogenesis.

Many studies have noted a positive correlation between centrosome amplification and advanced tumours, recurrence and poor survival [1, 2]. However the molecular basis for this has remained elusive. Very few studies have analysed the consequences of centrosome amplification *in vivo* in the context of a whole organism. In addition, the results reported were related to cell proliferation and survival and not to the consequences of centrosome amplification in differentiated cells of specific tissues [37-41]. Using cell culture systems, Godinho and coworkers have recently shown that centrosome amplification promotes cellular invasion, concluding that centrosome amplification can promote features of malignant transformation by altering the cytoskeleton [42]. Here we report that centrosome amplification increases branching in epithelial cells within a whole living organism. This occurs during a process similar to capillary sprouting of blood vessels during angiogenesis. Therefore, our findings shed more light on the consequences of centrosome amplification in differentiated cell behaviour and further strengthen the importance of cytoskeletal regulation during subcellular lumen formation, a process involved in angiogenic sprouting.

Supplemental Information

Supplemental Information includes Experimental Procedures, 4 figures and 4 movies.

Acknowledgements

We are grateful to M. Llimargas, V. Brodu and C. Gonzalez for comments on the manuscript. We thank F. Sprenger, M. Bettencourt-Dias, C. González and the Bloomington stock center for fly stocks and reagents. Thanks also go to L. Bardia, A. Lladó and J. Colombelli from the IRB-ADMF for assistance and advice with confocal microscopy and software; E. Fuentes, Y. Rivera and N. Martin for technical assistance; and G. Lebreton and L. Gervais for help and advice during early stages of this project. S.J.A. is a Ramon y Cajal Researcher (RYC-2007-00417); D.R. is the recipient of an FPU Ph.D. fellowship from the Spanish *Ministerio de Educación* (FPU12/O5765); M.D. was supported by the Erasmus Programme. This work was supported by the Generalitat de Catalunya and grants from the Spanish *Ministerio de Ciencia e Innovación/Ministerio de Economia y Competitividad* (BFU2009-07629 and BFU2012-32115). IRB Barcelona is the recipient of a Severo Ochoa Award of Excellence from MINECO (Spanish Government).

Author contributions

D.R., M.D. and S.J.A. performed all the experiments. D.R. and S.J.A. designed the experiments and analysed the data. J.C. provided expertise and feedback. S.J.A. conceived the study and wrote the paper.

References

1. Chan, J.Y. (2011). A clinical overview of centrosome amplification in human cancers. Int J Biol Sci *7*, 1122-1144.
2. Godinho, S.A., and Pellman, D. (2014). Causes and consequences of centrosome abnormalities in cancer. Philos Trans R Soc Lond, B, Biol Sci *369*.
3. Sigurbjörnsdóttir, S., Mathew, R., and Leptin, M. (2014). Molecular mechanisms of de novo lumen formation. Nat Rev Mol Cell Biol *15*, 665-676.
4. Samakovlis, C., Hacohen, N., Manning, G., Sutherland, D.C., Guillemin, K., and Krasnow, M.A. (1996). Development of the Drosophila tracheal system occurs by a series of morphologically distinct but genetically coupled branching events. Development *122*, 1395-1407.
5. Gervais, L., and Casanova, J. (2010). In vivo coupling of cell elongation and lumen formation in a single cell. Curr Biol *20*, 359-366.
6. Schottenfeld-Roames, J., and Ghabrial, A.S. (2012). Whacked and Rab35 polarize dynein-motor-complex-dependent seamless tube growth. Nature Cell Biology *14*, 386-393.
7. Schottenfeld-Roames, J., Rosa, J.B., and Ghabrial, A.S. (2014). Seamless Tube Shape Is Constrained by Endocytosis-Dependent Regulation of Active Moesin. Curr Biol *24*, 1756-1764.
8. Araújo, S.J., and Casanova, J. (2011). Sequoia establishes tip-cell number in Drosophila trachea by regulating FGF levels. Journal of Cell Science *124*, 2335-2340.
9. Grosskortenhaus, R., and Sprenger, F. (2002). Rca1 inhibits APC-Cdh1(Fzr) and is required to prevent cyclin degradation in G2. Dev Cell *2*, 29-40.
10. Tanaka-Matakatsu, M., Thomas, B.J., and Du, W. (2007). Mutation of the Apc1 homologue shattered disrupts normal eye development by disrupting G1 cell cycle arrest and progression through mitosis. Developmental Biology *309*, 222-235.
11. Reimann, J.D., Freed, E., Hsu, J.Y., Kramer, E.R., Peters, J.M., and Jackson, P.K. (2001). Emi1 is a mitotic regulator that interacts with Cdc20 and inhibits the anaphase promoting complex. Cell *105*, 645-655.
12. Dong, X., Zavitz, K.H., Thomas, B.J., Lin, M., Campbell, S., and Zipursky, S.L. (1997). Control of G1 in the developing Drosophila eye: rca1 regulates Cyclin A. Genes & Development *11*, 94-105.
13. Celniker, S.E., Dillon, L.A.L., Gerstein, M.B., Gunsalus, K.C., Henikoff, S., Karpen, G.H., Kellis, M., Lai, E.C., Lieb, J.D., MacAlpine, D.M., et al. (2009). Unlocking the secrets of the genome. Nature *459*, 927-930.
14. Sigrist, S.J., and Lehner, C.F. (1997). Drosophila fizzy-related down-regulates mitotic cyclins and is required for cell proliferation arrest and entry into endocycles. Cell *90*, 671-681.
15. Butí, E., Mesquita, D., and Araújo, S.J. (2014). Hedgehog Is a Positive Regulator of FGF Signalling during Embryonic Tracheal Cell Migration. PLoS ONE *9*, e92682.
16. Beitel, G.J., and Krasnow, M.A. (2000). Genetic control of epithelial tube size in the Drosophila tracheal system. Development *127*, 3271-3282.
17. Kondo, T., and Hayashi, S. (2013). Mitotic cell rounding accelerates epithelial invagination. Nature *494*, 125-129.
18. Prosser, S.L., Samant, M.D., Baxter, J.E., Morrison, C.G., and Fry, A.M. (2012). Oscillation of APC/C activity during cell cycle arrest promotes centrosome amplification. Journal of Cell Science *125*, 5353-5368.
19. Dienemann, A., and Sprenger, F. (2004). Requirements of cyclin a for mitosis are independent of its subcellular localization. Curr Biol *14*, 1117-1123.
20. Erhardt, S., Mellone, B.G., Betts, C.M., Zhang, W., Karpen, G.H., and Straight, A.F. (2008). Genome-wide analysis reveals a cell cycle-dependent mechanism controlling centromere propagation. The Journal of Cell Biology *183*, 805-818.

21. Bornens, M. (2012). The centrosome in cells and organisms. Science *335*, 422-426.
22. Bettencourt-Dias, M., Rodrigues-Martins, A., Carpenter, L., Riparbelli, M., Lehmann, L., Gatt, M.K., Carmo, N., Balloux, F., Callaini, G., and Glover, D.M. (2005). SAK/PLK4 is required for centriole duplication and flagella development. Curr Biol *15*, 2199-2207.
23. Cunha-Ferreira, I., Rodrigues-Martins, A., Bento, I., Riparbelli, M., Zhang, W., Laue, E., Callaini, G., Glover, D.M., and Bettencourt-Dias, M. (2009). The SCF/Slimb ubiquitin ligase limits centrosome amplification through degradation of SAK/PLK4. Curr Biol *19*, 43-49.
24. Rogers, G.C., Rusan, N.M., Roberts, D.M., Peifer, M., and Rogers, S.L. (2009). The SCF Slimb ubiquitin ligase regulates Plk4/Sak levels to block centriole reduplication. The Journal of Cell Biology *184*, 225-239.
25. Wojcik, E.J., Glover, D.M., and Hays, T.S. (2000). The SCF ubiquitin ligase protein slimb regulates centrosome duplication in Drosophila. Curr Biol *10*, 1131-1134.
26. Basto, R., Lau, J., Vinogradova, T., Gardiol, A., Woods, C.G., Khodjakov, A., and Raff, J.W. (2006). Flies without centrioles. Cell *125*, 1375-1386.
27. Wiese, C., and Zheng, Y. (2006). Microtubule nucleation: gamma-tubulin and beyond. Journal of Cell Science *119*, 4143-4153.
28. Brodu, V., Baffet, A.D., Le Droguen, P.-M., Casanova, J., and Guichet, A. (2010). A developmentally regulated two-step process generates a noncentrosomal microtubule network in Drosophila tracheal cells. Dev Cell *18*, 790-801.
29. Lin, T.-c., Neuner, A., and Schiebel, E. (2015). Targeting of γ-tubulin complexes to microtubule organizing centers: conservation and divergence. Trends in Cell Biology *25*, 296-307.
30. Chen, G., Rogers, A.K., League, G.P., and Nam, S.-C. (2011). Genetic interaction of centrosomin and bazooka in apical domain regulation in Drosophila photoreceptor. PLoS ONE *6*, e16127.
31. de Anda, F.C., Pollarolo, G., Da Silva, J.S., Camoletto, P.G., Feiguin, F., and Dotti, C.G. (2005). Centrosome localization determines neuronal polarity. Nature *436*, 704-708.
32. Pollarolo, G., Schulz, J.G., Munck, S., and Dotti, C.G. (2011). Cytokinesis remnants define first neuronal asymmetry in vivo. Nature Neuroscience *14*, 1525-1533.
33. Inaba, M., Venkei, Z.G., and Yamashita, Y.M. (2015). The polarity protein Baz forms a platform for the centrosome orientation during asymmetric stem cell division in the Drosophila male germline. eLife *4* e04960.
34. Shaye, D.D., and Greenwald, I. (2015). The disease-associated formin INF2/EXC-6 organizes lumen and cell outgrowth during tubulogenesis by regulating F-actin and microtubule cytoskeletons. Dev Cell *32*, 743-755.
35. Shi, X., Liu, M., Li, D., Wang, J., Aneja, R., and Zhou, J. (2012). Cep70 contributes to angiogenesis by modulating microtubule rearrangement and stimulating cell polarization and migration. Cell Cycle *11*, 1554-1563.
36. Yang, R., and Feldman, J.L. (2015). SPD-2/CEP192 and CDK Are Limiting for Microtubule-Organizing Center Function at the Centrosome. Curr Biol *25*, 1924-1931.
37. Basto, R., Brunk, K., Vinadogrova, T., Peel, N., Franz, A., Khodjakov, A., and Raff, J.W. (2008). Centrosome amplification can initiate tumorigenesis in flies. Cell *133*, 1032-1042.
38. Dzafic, E., Strzyz, P.J., Wilsch-Bräuninger, M., and Norden, C. (2015). Centriole Amplification in Zebrafish Affects Proliferation and Survival but Not Differentiation of Neural Progenitor Cells. CellReports *13*, 168-182.

39. Kulukian, A., Holland, A.J., Vitre, B., Naik, S., Cleveland, D.W., and Fuchs, E. (2015). Epidermal development, growth control, and homeostasis in the face of centrosome amplification. Proc Natl Acad Sci USA *112*, E6311-6320.
40. Vitre, B., Holland, A.J., Kulukian, A., Shoshani, O., Hirai, M., Wang, Y., Maldonado, M., Cho, T., Boubaker, J., Swing, D.A., et al. (2015). Chronic centrosome amplification without tumorigenesis. Proc Natl Acad Sci USA *112*, E6321-6330.
41. Marthiens, V., Rujano, M.A., Pennetier, C., Tessier, S., Paul-Gilloteaux, P., and Basto, R. (2013). Centrosome amplification causes microcephaly. Nat Cell Biol *15*, 731-740.
42. Godinho, S.A., Picone, R., Burute, M., Dagher, R., Su, Y., Leung, C.T., Polyak, K., Brugge, J.S., Théry, M., and Pellman, D. (2014). Oncogene-like induction of cellular invasion from centrosome amplification. Nature *510*, 167-171.

Figure legends

Figure 1. *Rca1* mutant embryos show tracheal TC branching phenotypes

(A - D) Tip of tracheal GBs at embryonic stage 16, displaying the tip and stalk cells and their lumina and stained for lumen (with CBP in red) and btlGFP in B and D to visualize tracheal cells (green), and DSRF to show the TC nucleus (green in A and C and blue in B and D). (A, B) wild-type TCs with a single lumen each; (C, D) *Rca1* mutant TCs showing subcellular lumen bifurcations. Scale bar represents 5 μm. See also Figure S1.

(E) Quantitation of the number of luminal bifurcations per embryo (± SEM) in various allelic combinations of *Rca1* and when *Rca1* is downregulated in tracheal cells by RNAi. (F) Quantitation of the population of embryos that show luminal bifurcations in various allelic combinations of *Rca1* and when *Rca1* is downregulated in tracheal cells by RNAi. wt n=41; $Rca1^{G012}$ n=52; $Rca1^{G012}/Rca1^{IX}$ n=56; $Rca1^{G012}/Df(2L)ED6569$ n=26; *btl>Rca1RNAi* n=17. See also Figure S1.

(G and H) Frames from movie S1, wt (G) and *Rca1* (H) showing several stages of subcellular lumen extension in the wild-type (G) and in *Rca1* mutant (H) GBs. The growing subcellular lumen extends from the cell-cell junction between the tip and stalk cell (asterisk). In the wild-type, only one subcellular lumen extends from the junction (G), whereas in the mutant two lumina extend from this point (H). Numbers on the lower right hand corner are minutes. See also Movie S1.

(I-R) Analysis of *Rca1* TC characteristics in comparison with wild-type TCs. (I, J, O, P) *Rca1* TCs grow lumina that structurally resemble the wild-type in lumen components such as chitin and Gasp/2A12 (N) or apical membrane markers

such as Baz (O). (K,P) Actin accumulates at the tip of the TC and the subcellular lumina grow in the direction of this actin-rich spot (arrows) both in wild-type (K) and *Rca1* TCs (P). (L, M, Q, R) *Rca1* TCs accumulate higher amounts of apical components such as aPKC (Q, asterisk) and Baz (R, asterisk). Scale bars represent 5 μm.

(S) Quantitation of Baz accumulation at the TC junction per embryo GB in wt (± SEM, n=5 embryos) and *Rca1* (± SEM, n=5 embryos). *Rca1* mutant embryos display an average of 5.6 TCs per embryo with higher Baz accumulation in contrast to 0.6 TCs in the wt (n=80 GB TCs).

(T-U) Tip of tracheal GBs at embryonic stage 16 displaying the tip and stalk *CycA* mutant cells stained for lumen (with CBP in red) in T and U and *btl>GFP* in U to visualize tracheal cells (green), and DSRF to show the TC nucleus (green in T and blue in U). *CycA* mutant TCs show subcellular lumen bifurcations. Scale bars represent 5 μm.

(V) Quantitation of the population of embryos that show luminal bifurcations in *Rca1* (n=52) in comparison with *CycA* mutant embryos (n=45).

Figure 2. Centriole amplification in *Rca1* and *CycA* mutant cells

(A and B) Centrioles observed in tracheal TCs at the stage of initiation of luminal elongation. (A) *Rca1* heterozygote and homozygote TCs stained for Asl to mark centrioles (green), btl::moeRFP to mark tracheal cells (Red) and DSRF to visualize the nucleus of the TC (blue); the white line marks the borders of the TC and the junction of the TC with the stalk cell. Note the higher numbers of centrioles in both *Rca1* mutant tracheal cells and in the surrounding tissues. (B) Quantitation of centrioles in heterozygote (± SEM; n= 33) and mutant *Rca1* TCs

(± SEM; n= 42).

(C and D) Centriole amplification observed after depletion of *Rca1* and *CycA* is at the same level as the one produced by depletion of *slmb*. (C) Cells were treated with dsRNA (indicated) and assayed for centriole numbers. CP309 (red) and DNA (blue). Scale bar represents 5 μm. (D) Quantitation of supernumerary centrioles after RNAi. Results were normalized relative to controls (ratio is equal to 1 in βGal controls). Data are the average of three RNAi experiments ± SEM (n = 200 cells in each experiment).

Figure 3. Centriole numbers affect subcellular lumen formation

(A - C) Tip of tracheal GBs at embryonic stage 16 displaying the tip and 2-3 stalk cells and their lumen, and stained with GFP to visualize tracheal cells (green), CBP to stain the tracheal chitinous lumen (red), and DSRF to show the TC nucleus (blue). (A) wild-type TCs with a single lumen each; (B) *slmb* mutant TCs showing subcellular lumen bifurcations; (C) *btl>SAKND*/SAKOE tracheal cells showing one cell with a luminal bifurcation and one wild-type TC lumen. See also Figure S2.

(D – F) *sas-4* mutant (E) and *Rca1;sas-4* double mutant (F) GB TCs compared to wild-type (D) TCs; stained with CBP to reveal the tracheal chitinous lumen (red) and DSRF to show the TC nucleus (blue). (E) *sas-4* mutant TCs have defects in subcellular lumen formation in 88% of all GB TCs (n= 19 embryos) (F) *sas-4* removal rescues the luminal bifurcation phenotype of *Rca1* mutant TCs. See also Figure S2.

(G) Quantitation of the population of embryos with bifurcations in the distinct genotypes. wt n=41; Rca1^{G012} n=52; *slmb* n=46; *btl>SAKND* n=50; *Rca1^{G012}*;*sas-4* n=35. See also Figure S2.

Figure 4. Centrosomes are MTOCs during the initiation of subcellular lumen formation

(A, B) Tracheal GBs at embryonic stage 14 (A) and stage 16 (B) showing the tip cells and their lumina, and stained with anti-GFP to visualize YFP centrioles (green) and *btl::moeRFP* to mark tracheal cells and the junction (arrow) between the tip and stalk cells (red). The two centrosomes in the TC localize near the tip-cell – stalk cell junction (circle in A'' and B''). *AslYFP* is expressed in all cells in the embryo and not just in the tracheal cells. Images are single confocal scans or projections of only 2-3 scans to include the whole terminal cell. Scale bars are 5 µm.

(C, D) Live frames showing *Rca1* heterozygous (C) and homozygous (D) embryos carrying constructs expressing Moe in all tracheal cells (*btl::moerfp*) and AslYFP in all cells. (C) *Rca1* heterozygous TC with 2 centrosomes near the apical cell-cell junction; (D) *Rca1* homozygous TC with 4 centrosomes localized apically.

(E,F) Progression of early stages of lumen formation in *Rca1* heterozygous (E) and homozygous (F) TCs carrying constructs expressing Moe (stained red), AslYFP (stained green) and stained for chitin to mark the growing lumen in blue. (E', F') confocal scans depicting only the lumen in white and centrosomes in cyan to show the relative positions of the centrosomes to the lumen; dotted

white line marks the TC borders; insets show only the lumen. Scale bars are 5 µm.

(G, H) Stable MTs in *Rca1* heterozygous (G) and homozygous (H) TCs carrying constructs expressing Moe (stained red), AslYFP (stained green) and stained acetylated MTs in blue. (G', H'') confocal scans depicting only the MT bundles; dotted black line marks the TC borders insets show MTs and centrosomes. Scale bars are 5 µm. See also Figure S4.

(I, J) Wild-type (I) and *Rca1* (J) TCs carrying the AslYFP construct and stained for YFP and γ-tubulin to show whether the apical TC centrosomes are active MTOCs; (I', J') higher magnification of (I, J) depicting how centrosomes colocalize with γ-tubulin; (I'', J'') only γ-tubulin staining. Note that the centrosome outside the TC does not colocalize with γ-tubulin in I'. Scale bars are 5 µm. See also Figure S4.

(K-R) Microtubule depolymerization-repolymerization assay in wt (K-N) and *Rca1* (O-R) mutant embryos. After a 6h incubation at 4°C (L, P), MTs are depolymerised (compare K, O with L, P, respectively); after 2min at room temperature (RT) (M, Q) MTs start regrowing from the centrosome pair in the wt and the 4 centrosomes in *Rca1*, near the apical junction of the TC; after 30 min at RT (N, R) MTs have fully regrown from the centrosomes. Centrioles are detected by the Asl-YFP transgene, MTs are detected by a α-tubulin antibody. Scale bars are 2 µm.

(S) Graphical representation of our findings and the involvement of centrosomes in subcellular lumen formation in wild-type tracheal TCs. Straight arrows indicate time progression and dotted arrows cell migration. (T) Graphical

representation of our findings and the involvement of centrosomes in subcellular lumen formation in tracheal TCs with supernumerary centrosomes.

Figure 1

Click here to download Figure Fig.1.tif

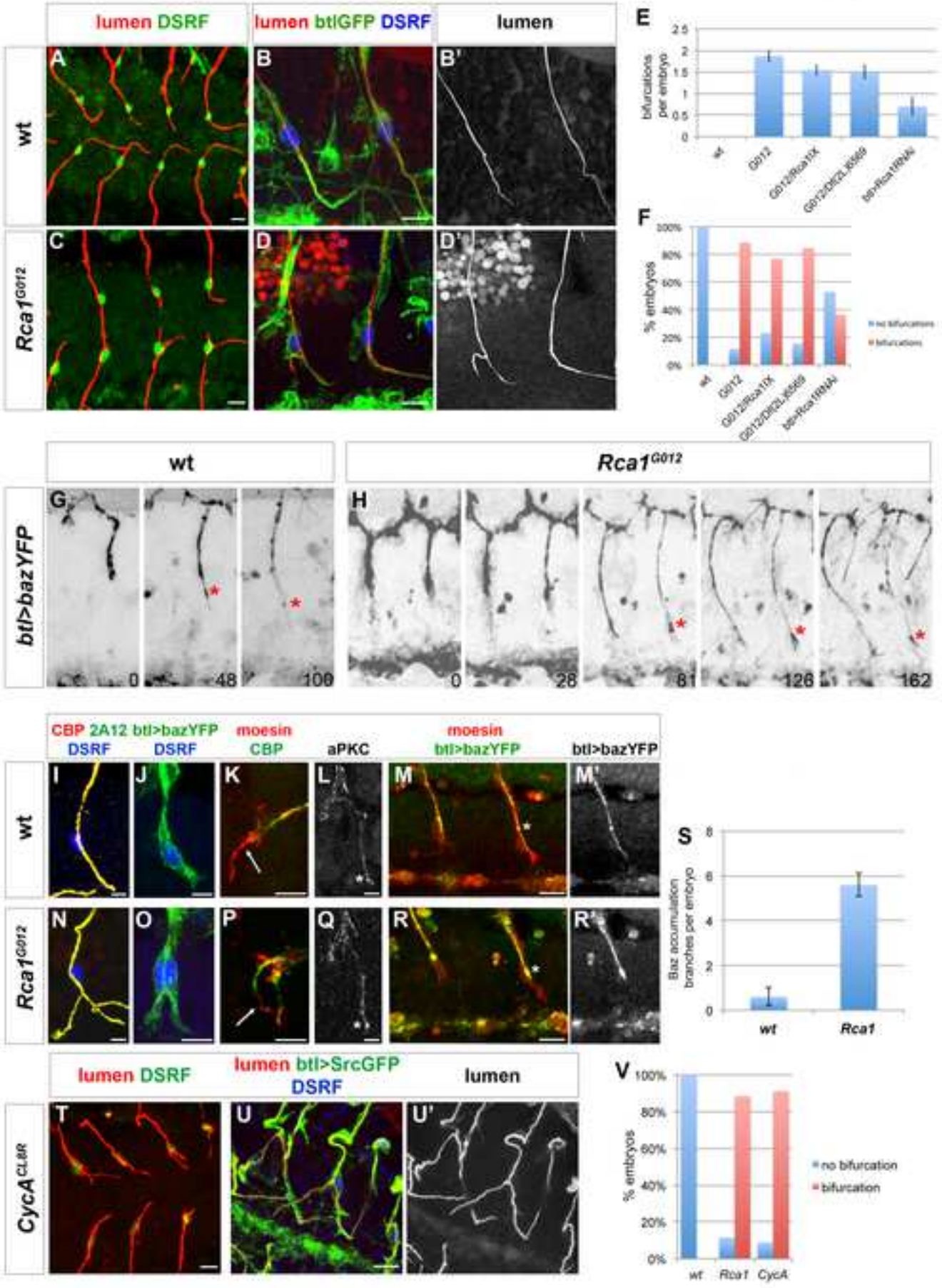

Figure 2

Click here to download Figure Fig.2.tif

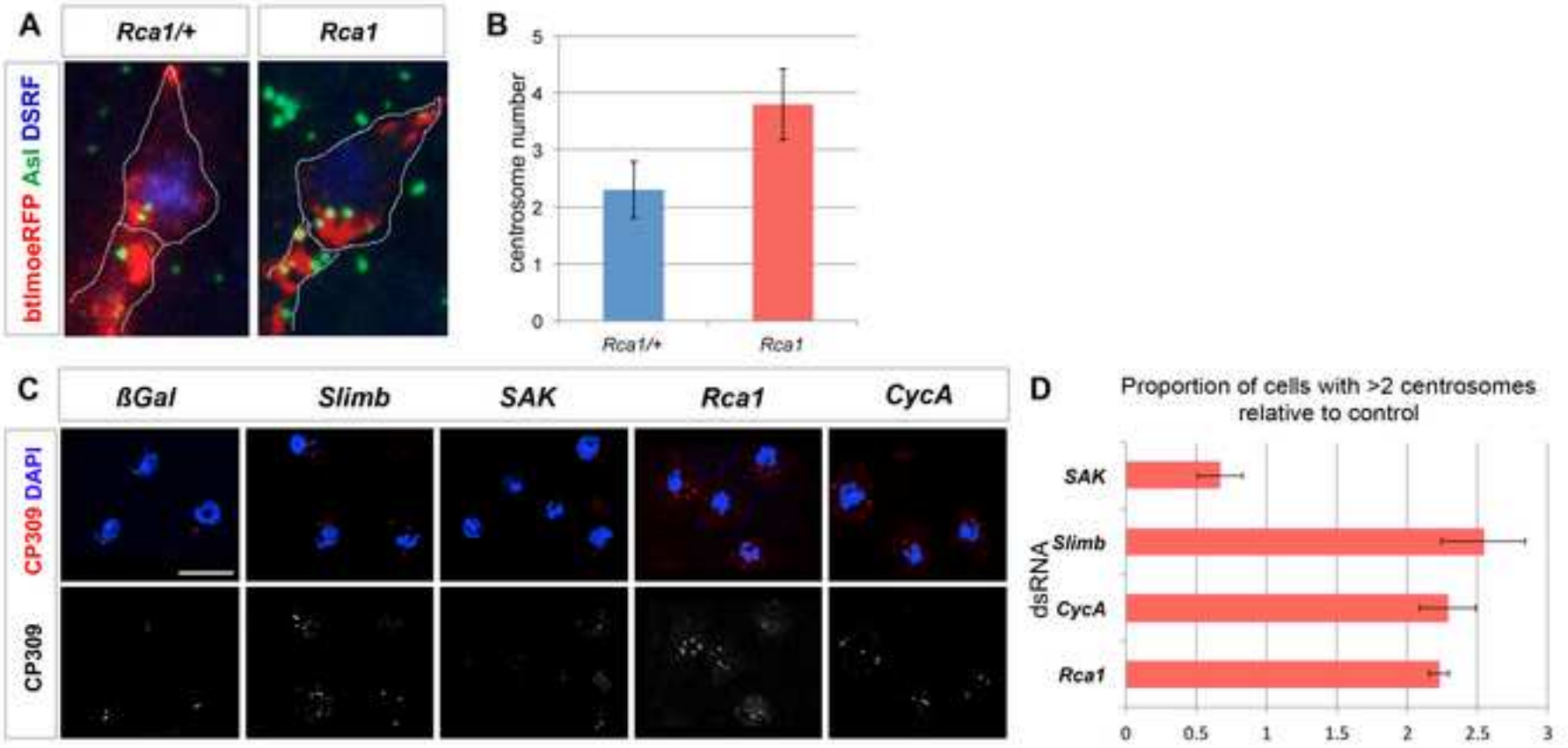

Figure 3

Click here to download Figure Fig.3.tif

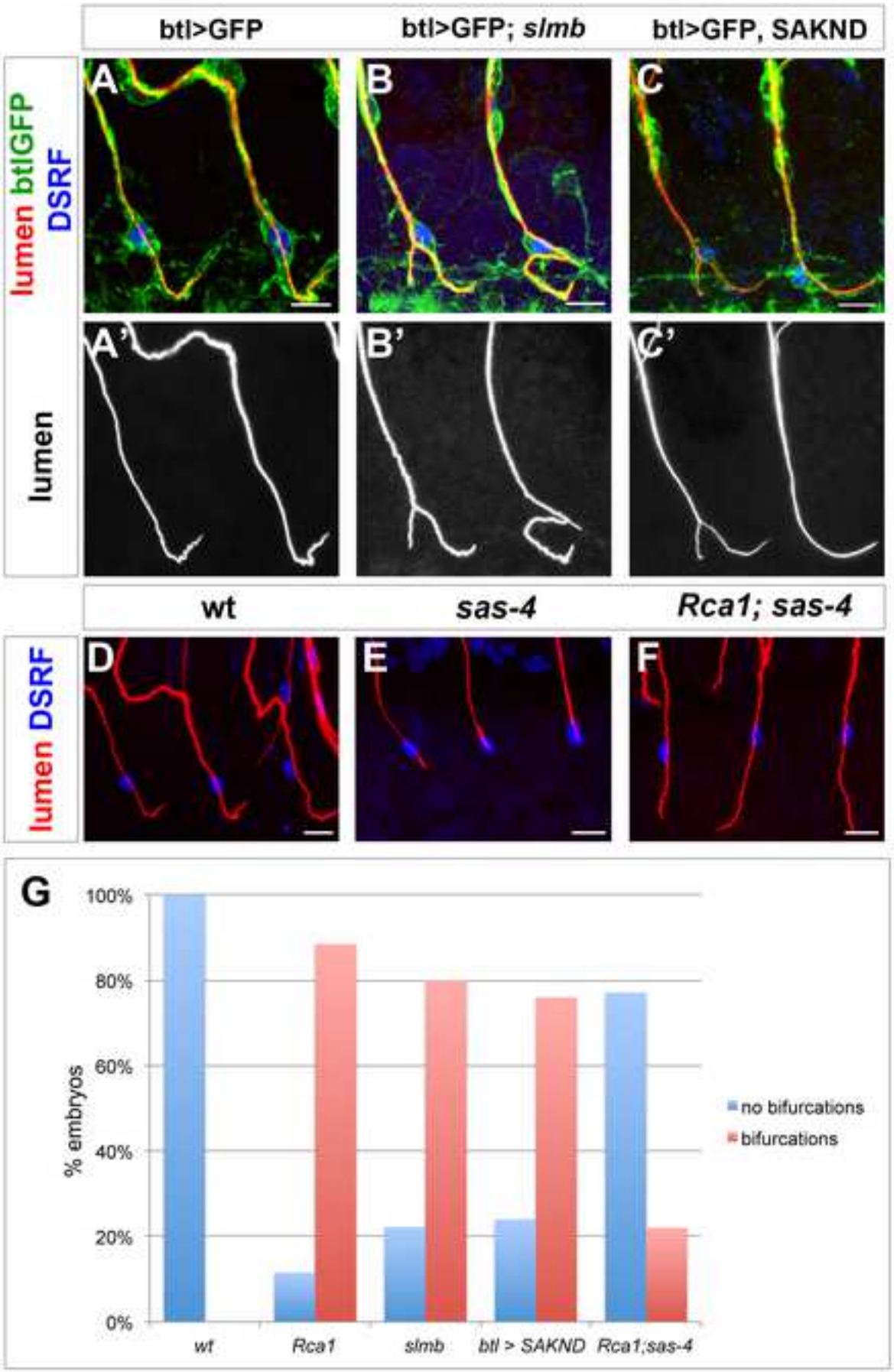

Figure 4

Click here to download Figure Fig.4.tif

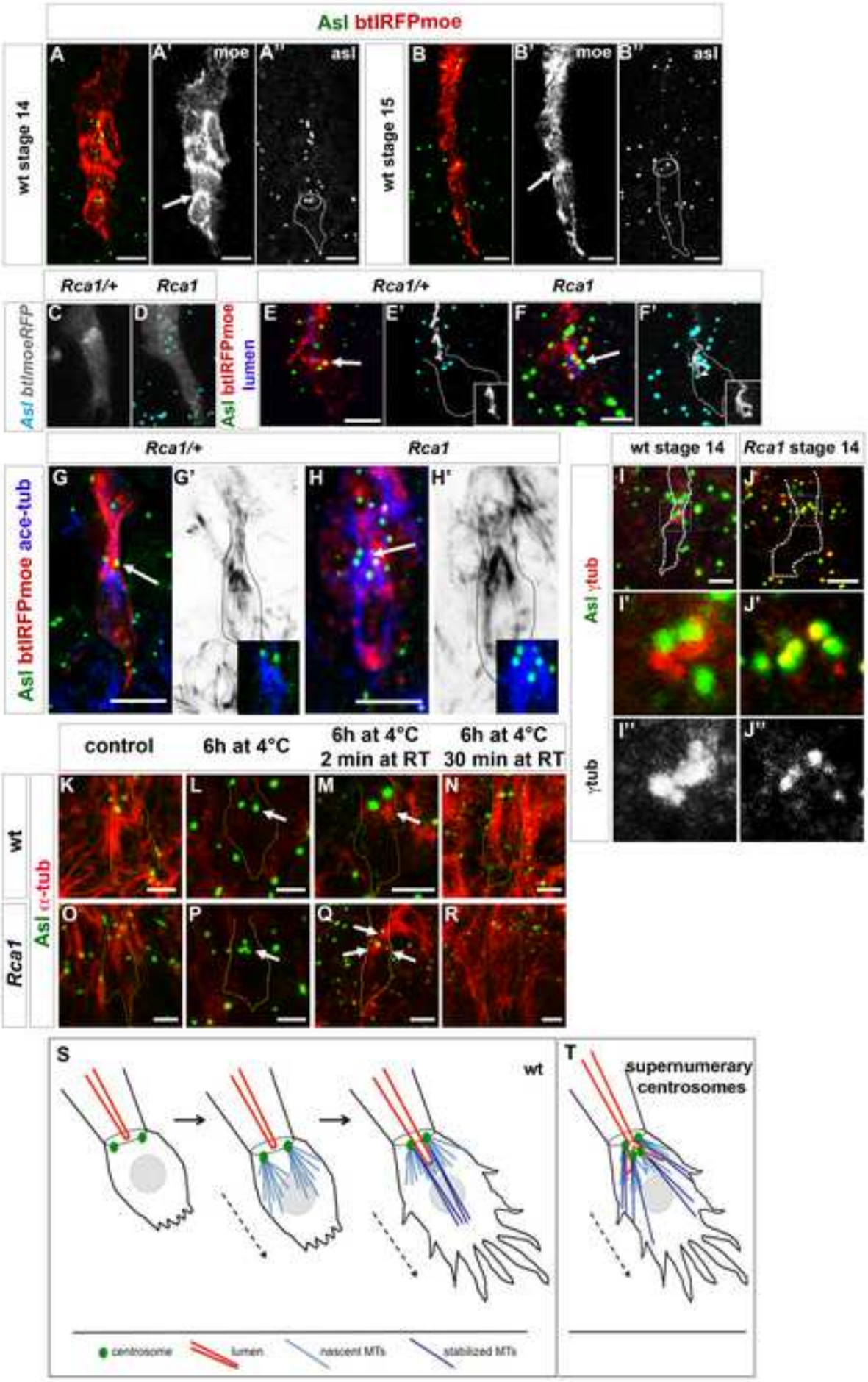

Supplemental Figures

Figure S1 - Related to Figure 1

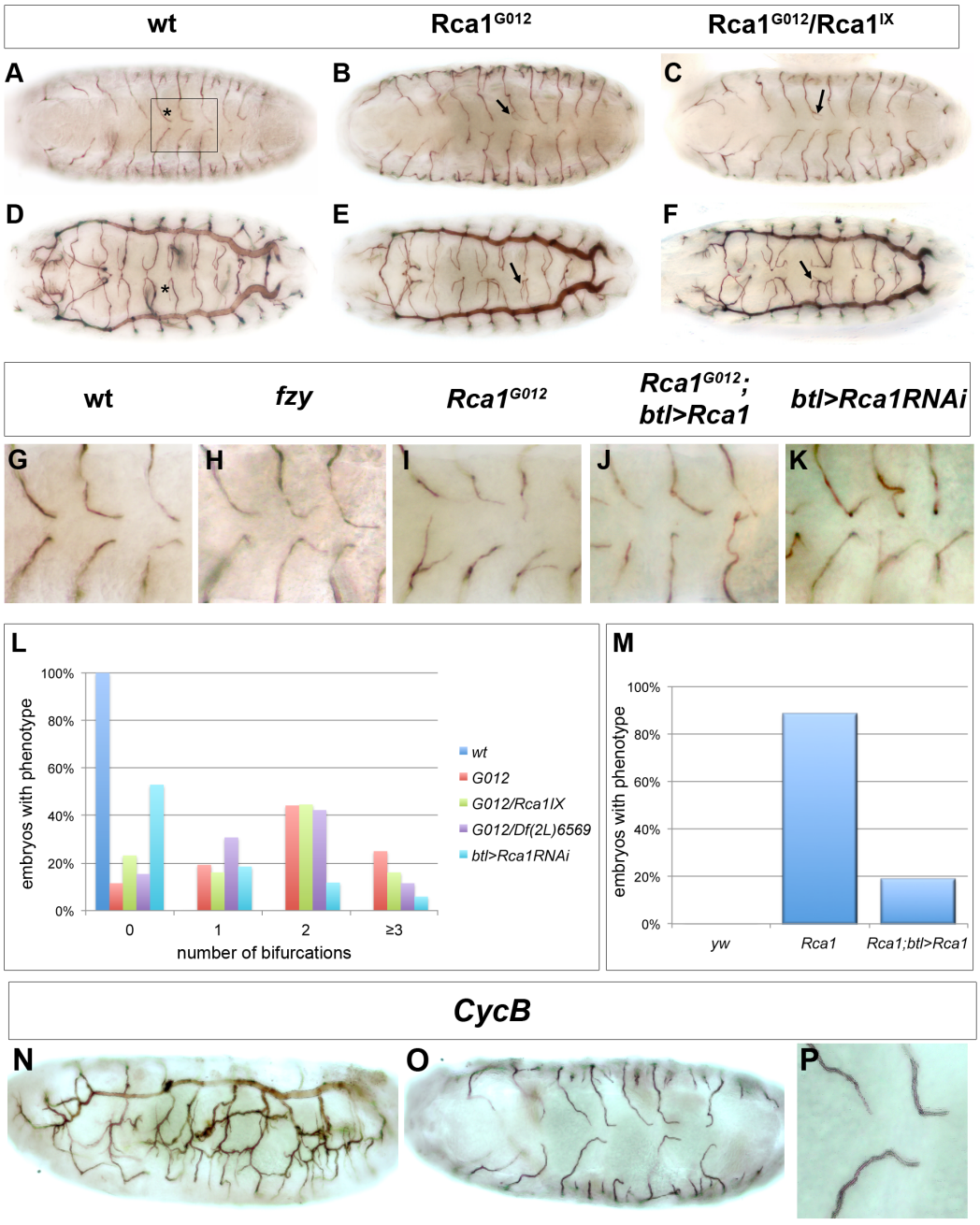

Figure S1. Related to Figure 1– *Rca1* mutant alleles display extra subcellular lumen (bifurcation) phenotypes

(A) Ventral view of a wt stage 16 embryo stained with 2A12 and showing the ganglionic braches (GBs). In the wt, each terminal cell of each GB, extends only one subcellular lumen (asterisk); (B) Ventral view of a *Rca1*^{G012} homozygous stage 16 embryo stained with 2A12 (anti-Gasp) and showing the extra subcellular branching phenotypes displayed by the GB terminal cells (arrow); (C) Ventral view of a *Rca1*^{G012}/*Rca1*^{IX} stage 16 embryo stained with 2A12 and showing the extra subcellular branching phenotypes displayed by the GB terminal cells (arrow); (D) Dorsal view of a wt stage 16 embryo stained with 2A12 and showing the dorsal braches (DBs). In the wt, each terminal cell of each DB, extends only

one subcellular lumen (asterisk); (E) Dorsal view of a *Rca1*^{G012} homozygous stage 16 embryo stained with 2A12 and showing the extra subcellular branching phenotypes displayed by the DB terminal cells (arrow); (F) Dorsal view of a *Rca1*^{G012}/*Rca1*^{IX} stage 16 embryo stained with 2A12 and showing the extra subcellular branching phenotypes displayed by the DB terminal cells (arrow).
(G) Magnified region (see square in A) of the ventral side of stage 16 wt embryo, showing GB lumina in detail; (H) same region in a *fzy* homozygous embryo; (I) *Rca1*^{G012} embryo; (J) *Rca1*^{G012} embryo rescued by the expression of a full length Rca1 construct driven in tracheal cells (*btl* positive cells); (K) Detail of an embryo where Rca1 was downregulated by means of *Rca1RNAi* expression in tracheal cells.
(L) Quantification of the number of extracellular lumen events found per embryo in each of the allelic combinations tested. We counted the number of extracellular lumen events per embryo and results are presented in percentage of embryos displaying each of the phenotypes. wt n=41, *Rca1*^{G012} n=52, *Rca1*^{G012}/*Rca1*^{IX} n=56, *Rca1*^{G012}/*Df(2L)6569* n=26, *btl>Rca1RNAi* n=17. We did not differentiate between number of extracellular lumina per terminal cell (i.e. more than one lumen per cell was quantified as a bifurcation as these represented the majority of cases).
(M) Percentage of embryos with extra subcellular lumen phenotypes in the wt (n=41) and *Rca1*^{G012} (n=52) compared with *Rca1* rescued embryos. The expression of a full length *Rca1* construct in tracheal cells from stage 11, rescues the terminal bifurcation phenotypes in 81% of the embryos analysed (n=32).
(N-P) *CycB* mutant embryos do not develop luminal bifurcations in TCs. (N) Lateral view of a stage 16 *CycB* embryo showing branching phenotypes in multicellular tracheal branches; (O) Ventral view of the same stage 16 *CycB* embryo showing GB phenotypes such as lack of 2A12 staining in some GBs, but no apparent bifurcations; (P) Magnified ventral region of another stage 16 *CycB* embryo showing the tips of the GBs and the single lumina of the TCs.

Figure S2 - Related to Figure 3

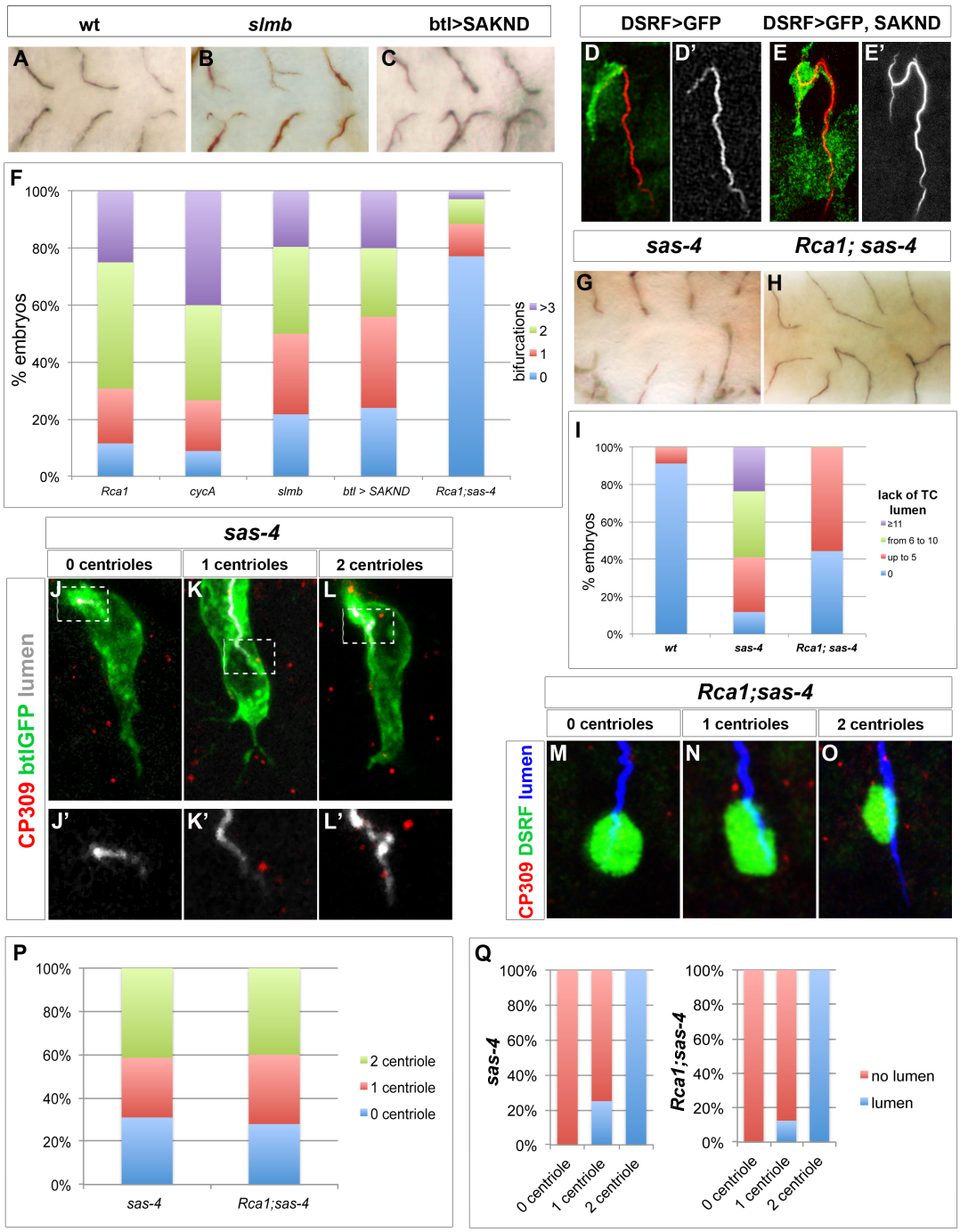

Figure S2. Related to Figure 3 - Centrosome number is directly linked to subcellular lumen extension

(A-C) Magnified region (see square in S1 A) of the ventral side of stage 16 embryos, showing GB lumina in detail. (A) wt; (B) *slmb* mutant; (C) *wt* embryo carrying a SAKND construct driven in all tracheal cells (*btl* positive cells) from stage 11 – tracheal cell SAKOE.

(D-E) Detail of a DB showing the TC in green due to the expression of GFP in DSRF expressing cells only. (D) Expression of a UASGFP; (E) Expression of a UASSAKNDGFP – TC SAKOE.

(F) Quantification of the percentage of embryos of the genotypes described in the x-axis, which display none, 1, 2 or more than 3 bifurcations. $Rca1^{G012}$ n=52, $CycA^{CL8R1}$ n=45, $slmb^{00295}$ n=46, *btl>SAKND* n=50, $Rca1^{G012}$;$sas\text{-}4^{2214}$ n= 35 embryos.

(G-H) Magnified region of the ventral side of stage 16 embryos, showing GB lumina in detail. (G) *sas-4* mutant; (H) *Rca1;sas-4* double mutant; double mutants show a clear rescue of the bifurcation phenotypes of *Rca1*, despite still showing guidance phenotypes.
(I) Quantification of *sas-4* and *Rca1;sas-4* lack of TC lumina phenotypes and comparison with the wt. *sas-4* mutant luminal phenotypes are very variable, ranging from none (wt-like) to very few TCs without lumen to nearly all the embryonic GB TCs displaying no subcellular lumina. In the case of the double mutant, embryos range from no TC lumen to about half of the GBs not displaying subcellular lumina.
(J-L) Detail of *sas-4* GB TCs at stage 16. (J) TC with no centrosome; (K, K') TC with only one centrosome (arrow in K'); (L, L') TC with 2 centrosomes (arrows in L'); please note how TCs have already extended in all cases and only in (L, L') there is the beginning of a subcellular lumen (asterisk in L').
(M-O) Detail of *Rca1;sas-4* double mutant GB TCs at stage 16. (M) TC with no centrosome; (N) TC with only one centrosome (arrow); (O) TC with 2 centrosomes (arrows); only in (O) there is the formation of a subcellular lumen (asterisk).
(P) Quantitation of centriole number per TC in *sas-4* mutants (n=29) and *Rca1;sas-4* double mutants (n=25). In *Rca1;sas-4* double mutants centrioles vary from 0 to 2 per TC, rescuing the supernumerary centrosome phenotype of *Rca1* mutant embryos.
(Q) Correlation of the number of centrioles per TC in *sas-4* mutants (n=29) and *Rca1;sas-4* double mutants (n=25). In both cases, we found that all TCs analysed that display no centrioles do not extend a subcellular lumen, whereas mutant cells with 2 centrioles extend a subcellular lumen.

Figure S3 - Related to Figure 3

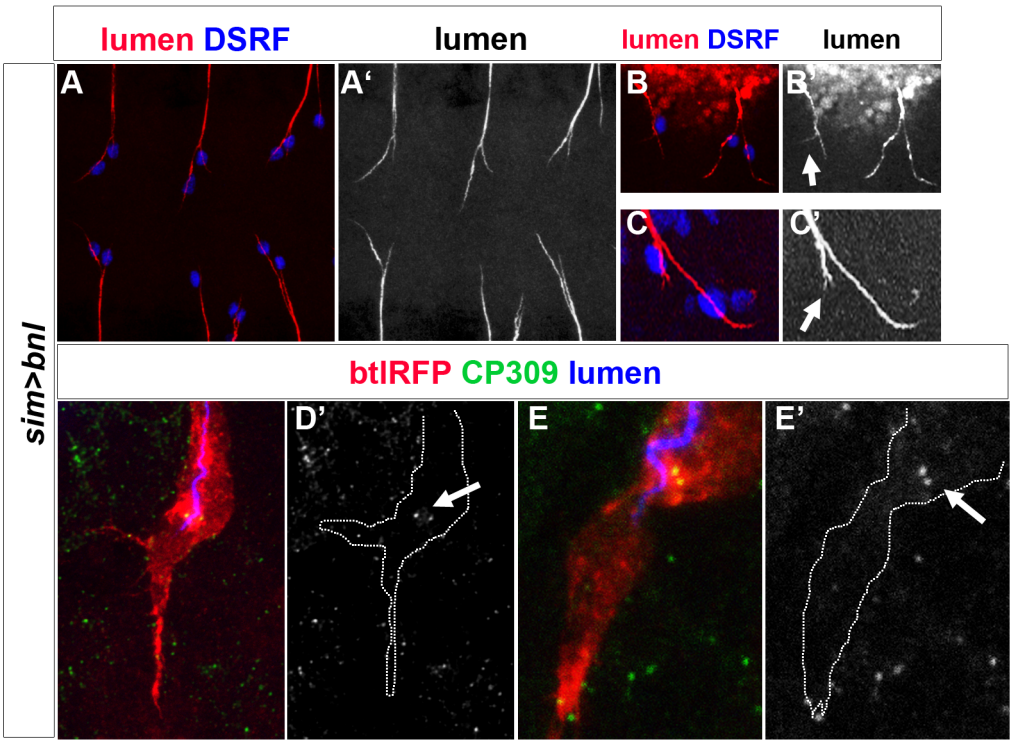

Figure S3. Related to Figure 3 – Activation of FGFR in embryonic stages does not lead to supernumerary centrosomes

Since branching is physiologically induced upon hypoxia, we addressed whether centrosome amplification was required in these conditions. One consequence of hypoxia is the upregulation of FGFR activity in the tracheal system, therefore we questioned if centrosome amplification could be detected upon FGFR overactivation. We and others have analysed the consequences of *bnl* overexpression (condition that mimics hypoxia by upregulating FGFR activity in tracheal cells) in tissues surrounding the GB TCs (midline cells). These conditions increased GB branching mainly by increasing the numbers of tip cells in the GBs [S1]. We have quantified the number of times we could detect TCs with extra subcellular lumina.

(A) Detail of a ventral region of a stage 16 embryo where FGFR (*Btl*) has been overactivated in tracheal cells by expression of its ligand FGF (*Bnl*) in the midline. Please not all bifurcations generated by 2 tip cells (TCs are detected by DSRF nuclear expression). We analysed 96 GBs and could only detect 2 with extra subcellular lumina in contrast with 43 that display bifurcations generated by 2 TCs.

(B,C) Detail of 2 TCs where 2 subcellular lumina are generated within the same TC (arrows). In the few cases where a subcellular lumen bifurcation is generated inside one TC, these bifurcations are quite incipient and different from the ones generated by centrosome amplification, as they seem to emanate not from the apical junction but from the TC lumen itself (arrows).

(D,E) Detail of 2 TCs where FGFR (*Btl*) has been overactivated by expression of its ligand FGF (*Bnl*) in the midline. Centrosomes are marked in green (arrows in D' and E') and lumen in blue. As in the examples presented here, in all cases analysed (n=16), we could not detect any supernumerary centrosomes. This suggests that subcellular lumen branching upon overactivation of FGFR does not seem to be dependent on centrosome amplification, at least during embryonic stages.

Figure S4 - Related to Figure 4

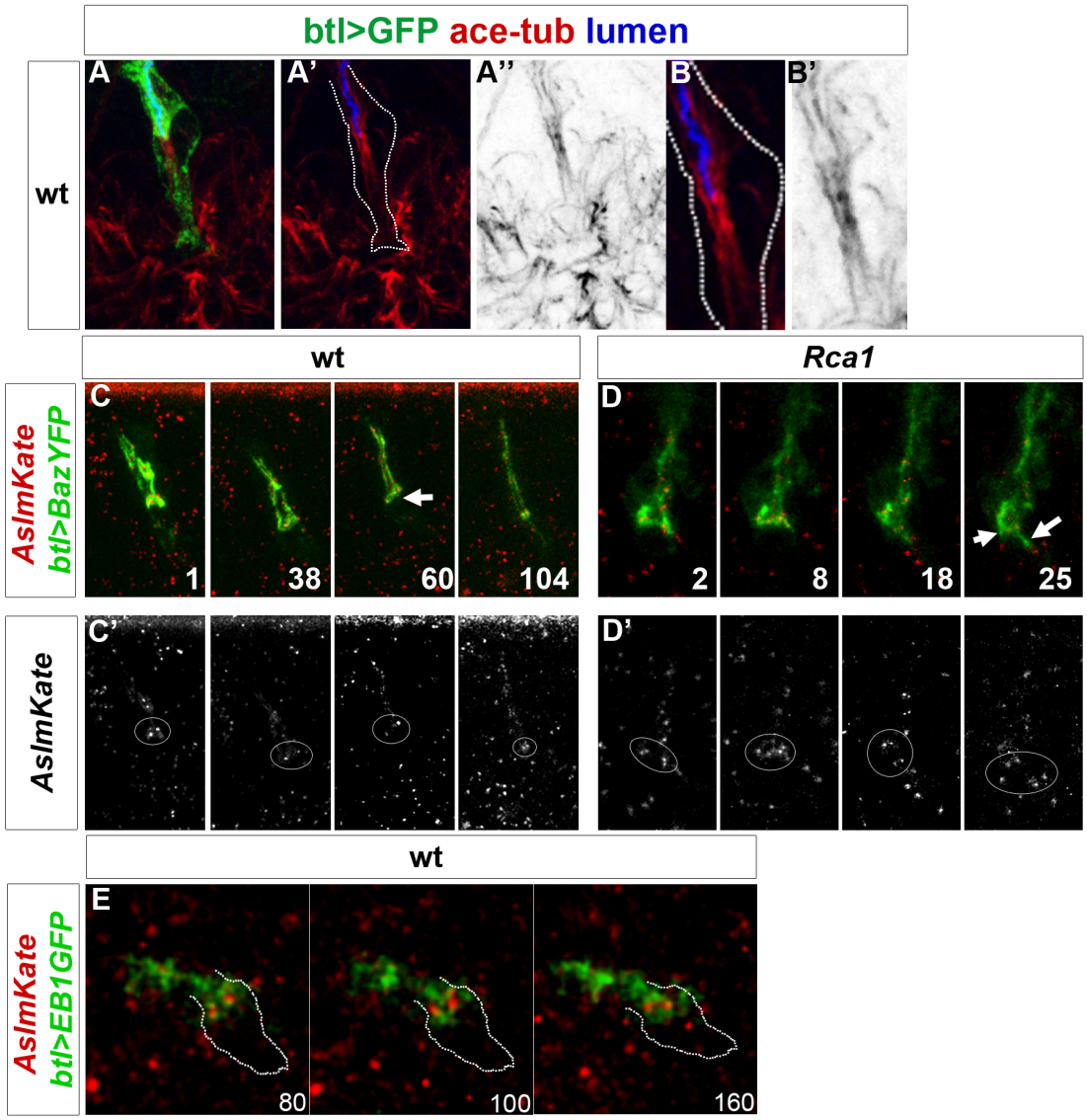

Figure S4. Related to Figure 4 – Two MT tracks are formed on each side of the ingrowing lumen in association with the centrosomes

(A,B) Detail of a TC stained in green due to the expression of GFP in *btl* expressing cells with marked MTs (acetylated-tubulin) in red and the lumen (CBP) in blue. B is a close-up of A.

(C-D) Frames from Movie S3 wt (C) and *Rca1* (D) showing several stages of subcellular lumen extension in the wild-type (C) and in *Rca1* mutant (D) GBs. Flies carry a construct that marks all centrioles in the embryo (AslmKate) and another that labels Baz only in tracheal cells (btl>bazYFP). The growing subcellular lumen extends from the cell-cell junction between the tip and stalk cell (white arrows). In the wild-type, only one subcellular lumen extends from the junction (C), whereas in the mutant two lumina extend from this point (D). Centrosomes associate with Baz at the cell-cell junction. In (C) 2 centrosomes are associated with the TC apical junction and in (D) 4 centrosomes are associated with the TC apical junction. Numbers on the lower right hand corner are minutes. White circles mark the region where TC centrosomes localize in each frame. See also Movie S3.

(E) Frames from Movie S4 showing initiation of subcellular lumen extension in wild-type GB. Flies carry a construct that marks all centrioles in the embryo (AslmKate) and another that labels EB1 only in tracheal cells (btl>EBI1GFP). The centrosomes at the apical junction of the TC associate with EB1. Numbers on the lower right hand corner are seconds. White line marks the TC membrane. See also Movie S4.

Supplemental Experimental Procedures

***Drosophila* strains and genetics**

All *D. melanogaster* strains were raised at 25°C under standard conditions. Mutant chromosomes were balanced over LacZ or GFP-labelled balancer chromosomes. Overexpression and rescue experiments were carried out either with *btlGAL4 (*M. Affolter) or *trhGAL4 (*Bloomington Stock Center [S2]) drivers at 25°C or 29°C. y^1w^{118} (wild-type), $rca1^{IX}$, $rca1^2$, $CycA^{C8LR1}$, $slmb^{0295}$, $Sas\text{-}4^{2214}$, *UAS-SrcGFP, simGAL4* and *UAS-slmb-RNAi* are described in FlyBase. *UAS-Rca1RNAi* (VDRC), *UAS-SAKND* (M. Bettencourt-Dias), *UAS-Rca1* (F. Sprenger), *UAS-bazYFP* (L. Gervais), *Asl::YFP* and *Asl::m-Kate* (C. Gonzalez), *btl::MoeGFP* (S. Hayashi), *btl::MoeRFP (M. Affolter)*, *UAS-EB1GFP* (A. Guichet), *UASbnl* (M. Krasnow) and $Rca1^{G012}$ (this work).

Immunohistochemistry, image acquisition and processing

Standard protocols for immunostaining were applied. The following antibodies were used: rat anti-DE-cad (DCAD2, DSHB); rabbit and rat anti-DSRF (J. Casanova); mouse anti-Crb (Cq4, DSHB) goat anti-GFP (AbCAm) rabbit anti-GFP (Molecular Probes); mAb2A12 (DSHB); rabbit anti-dRip11 (J. Casanova); mouse anti-acetylated-tubulin (Sigma), mouse anti-alpha-tubulin (DM1A, Thermofisher) rabbit anti-gamma-tubulin (C. Gonzalez) and chicken anti-β-gal (Cappel). Biotinylated, Cy3-, Cy2- and Cy5-conjugated secondary antibodies (Jackson ImmunoResearch) or Alexa conjugated secondary antibodies (Thermofisher) were used at 1:250. For some fluorescent stainings, the signal was amplified using TSA (NEN Life Sciences) when required. Chitin was visualised with CBP. Confocal images of fixed embryos were obtained either with a Leica TCS-SPE or a Leica TCS-SP5 system. Images were processed using Fiji and assembled using Photoshop.

Constructs, RNAi and Cell Lines

dsRNA against SAK, slmb, Rca1 and CycA was made from genomic and plasmid DNA and transfected into *Drosophila* S2 [S3]. A list of primer pairs can be found in Table S1. *Drosophila* S2 cells were cultured and transfected with 40 mg of dsRNA and 20 ml of Transfast (Promega) in 6-well plates. Cells were harvested after 4 days unless otherwise indicated.

List of primers used

RNAi primers	Forward	Reverse
CYCA	TAATACGACTCACTATAGGGAGATTTCACGTCATGGTTCTCTT	TAATACGACTCACTATAGGGAGGCCAAGAAATCGAATGTGGT
RCA1	TAATACGACTCACTATAGGGAGGCCTCGCTTATGAAAACCC	TAATACGACTCACTATAGGGAGTTTCAATCGCCACACAGTAG
SLMB	TAATACGACTCACTATAGGGAGAGCACAGGCCTTCACAACCACTATG	TAATACGACTCACTATAGGGAGTTGCAGACCAGCTCGGATGATTT
SAK	TAATACGACTCACTATAGGGAGAATACGGGAGGAATTTAAGCAAGTC	TAATACGACTCACTATAGGGAGATTATAACGCGTCGGAAGCAGTCT

Quantitative Analysis

For quantification of centrosome numbers in S2 cells after RNAi experiments, a total of 200 cells were scored per sample per slide. Cells were categorized according to number of centrosomes present (1, 2, 3, 4 or more than 4). Data shown are an average of 3 independent experiments.

The number of centrosomes per terminal cell in wild type, *Rca1* and *CycA* mutant embryos was counted in fixed and stained samples of stage 14 embryos.

The number of supernumerary terminal branches *per* terminal cell in wild type, *Rca1*, *CycA*, *slmb*, *sas-4*, *rca1*;*sas-4* and SAKOE embryos was manually counted in fixed and stained samples of stage 16-17 embryos.

Student T-tests were used to determine whether phenotypes were significant.

Time-lapse imaging

Dechorionated embryos were immobilised with glue on a coverslip and covered with Oil 10-S Voltalef (VWR). To visualise centrosomes *in vivo*, *Asl::YFP and Asl::m-Kate* were used in the indicated backgrounds. Tracheal cells were visualised with *btl::moeRFP* or *btlGAL4UASsrcGFP* where indicated.

Imaging was done with a spectral confocal microscope Leica TCS SP5. The images were acquired every 3 or 4 mins in Movies 1 and 2 over 50-75 µm from stage 14-15 embryos for 2–3 h. and every 10-38 secs in movies 3-6 over 50-75 µm from stage 14-15 embryos for 1–2 h. Frames are results of maximum projections. The movies were assembled using Fiji [S4].

Supplemental References

S1. Araujo, S.J., and Casanova, J. (2011). Sequoia establishes tip-cell number in Drosophila trachea by regulating FGF levels. J Cell Sci *124*, 2335-2340.

S2. Jenett, A., Rubin, G.M., Ngo, T.-T.B., Shepherd, D., Murphy, C., Dionne, H., Pfeiffer, B.D., Cavallaro, A., Hall, D., Jeter, J., et al. (2012). A GAL4-Driver Line Resource for Drosophila Neurobiology. CellReports. *2*, 991-1001

S3. Bettencourt-Dias, M., Giet, R., Sinka, R., Mazumdar, A., Lock, W.G., Balloux, F., Zafiropoulos, P.J., Yamaguchi, S., Winter, S., Carthew, R.W., et al. (2004). Genome-wide survey of protein kinases required for cell cycle progression. Nature *432*, 980-987.

S4. Schindelin J, A.-C.I., Frise E, Kaynig V, Longair M, Pietzsch T, Preibisch S, Rueden C, Saalfeld S, Schmid B, Tinevez JY, White DJ, Hartenstein V, Eliceiri K, Tomancak P, Cardona A. (2012). Fiji: an open-source platform for biological-image analysis. Nat Methods *9*, 676-682.